PHYSICAL REVIEW C VOLUME 23, NUMBER 1 JANUARY 1981

# Inclusive ($\pi^{\pm}$,$\pi^0$) reactions in nuclei

T. J. Bowles,* D. F. Geesaman, R. J. Holt, H. E. Jackson, J. Julien,† R. M. Laszewski,‡ J. R. Specht, and E. J. Stephenson§
*Argonne National Laboratory, Argonne, Illinois 60439*

R. P. Redwine
*Massachusetts Institute of Technology, Cambridge, Massachusetts 02139*

L. L. Rutledge, Jr‖ and R. E. Segel
*Northwestern University, Evanson, Illinois 60201*

M. A. Yates
*Los Alamos Scientific Laboratory, Los Alamos, New Mexico 87545*
(Received 27 May 1980)

Nuclear pion single-charge exchange has been studied using a method of $\pi^0$ detection based on the spectroscopy of the back-angle $\gamma$-ray decay. Charge-exchange scattering from nuclei ranging from Be to Pb was studied for incident pion energies of 50 and 100 MeV. The angular distributions and $\pi^0$ energy spectra beyond 60° suggest effects characteristic of quasifree scattering. Total charge-exchange cross sections are larger than values suggested by optical-model calculations.

[NUCLEAR REACTIONS $^{9}$Be, $^{12}$C, $^{16}$O, $^{58}$Ni, $^{208}$Pb ($\pi^{\pm}$,$\pi^0$) $E_{\pi}$ = 50 and 100 MeV, $\theta_{\pi^0}$ = 25, 40, 60, 90, 120, 150°; measured $d^2\sigma/d\Omega dE$ for $0 < E_{\pi^0} < E_{\pi^{\pm}}$.]

## I. INTRODUCTION

Simple inclusive particle spectra from pion induced reactions can provide valuable information on the general properties of pion nucleus interactions and rigorous tests of models of such reactions. Among the simplest and most important questions to be answered is the manner in which the total pion nucleus interaction is partitioned between elastic and inelastic scattering, pion single-charge exchange, and "true absorption." The available data are still fragmentary. In recent experiments[1] the absorption cross section has been determined by comparing empirical pion scattering cross sections with related transmission cross sections. To obtain these data the authors were compelled to estimate the charge-exchange contribution by scaling the measured pion scattering data with free pion nucleon cross sections. Almost no experimental data exist on the general features of single-charge-exchange reactions such as the total cross section[2] and its variation with $A$, the $\pi^0$ energy spectra and its dependence on scattering angle, or the angular distribution of the energy integrated cross section. Such information can provide valuable insights into the reaction mechanism. It is often assumed that the dominant process in pion scattering is scattering from single weakly interacting nucleons, i.e., quasifree scattering. Alternatively, inelastic and charge-exchange transitions to bound final states (quasielastic scattering) may be important. The angular distributions and energy spectra can clarify the relative importance of quasifree scattering reactions. Direct measurements of single-charge-exchange reactions over the full range of momentum transfer can determine the contribution of this process to the total reaction cross section, and clarify the importance of single-charge exchange in the propagation of pions in nuclear matter. In addition, reliable estimates of quasifree charge-exchange cross sections can provide useful constraints on optical model potentials used to describe pion nucleus scattering. Since single-charge exchange is generated by the isovector component of the $\pi$-nucleon reaction, it may be an effective probe for studying the isospin structure of the $\pi$-nucleus interaction.

In this paper we report the results of a series of measurements in which nuclear pion single-charge-exchange reactions have been studied using a method of $\pi^0$ detection[3] based on the spectroscopy of the back-angle decay $\gamma$ ray. Although the technique is not capable of the high resolution necessary to resolve individual states, it does permit the observation of scattering involving excitations averaged over $\pi^0$ energy intervals of approximately 5 MeV. Charge-exchange scattering using this technique has been employed to study nuclei ranging from Be to Pb for incident pion energies of 50

 

and 100 MeV. The data show that the angular distributions and $\pi^0$ energy spectra beyond 60° are dominated by effects characteristic of quasifree scattering. Total charge-exchange cross sections determined from these data are found to be larger than the values suggested by optical-model calculations.

## II. EXPERIMENTAL METHOD

The principle of the technique employed to study the inclusive $\pi^0$ spectra can be demonstrated from the kinematics for $\pi^0$ decay shown in Figs. 1 and 2. In Fig. 1 the decay-photon energy contours are given as a function of the opening angle between the two photons. The photon emission angle relative to the $\pi^0$ momentum for the high energy decay photon is shown in Fig. 2 as a function of the photon opening angle. In the actual experiment the detector geometry is arranged in order to restrict decay opening angles to values near 180°. The technique takes advantage of the fact that the $\pi^0$ decay photons emitted at back angles are strongly Doppler shifted to lower energies. As indicated in Fig. 1, for $\pi^0$ energies between 50 and 200 MeV, the corresponding decay-photon energies for photons emitted at 180° will range from 30 to 15 MeV, respectively. These backward-emitted photons can be observed in large volume NaI(Tl) spectrometers and their energy spectrum used to deduce the $\pi^0$ energy spectrum. From Fig. 2 it is evident that for opening angles between the decay photons greater than ≈170° and $\pi^0$ energies above 20 MeV, the angle between the high-energy decay photon

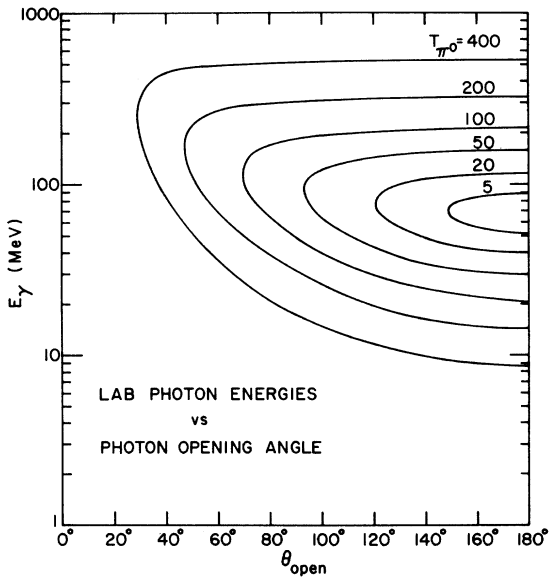


FIG. 1. Contours of decay photon energy as a function of photon opening angle for various $\pi^0$ kinetic energies.

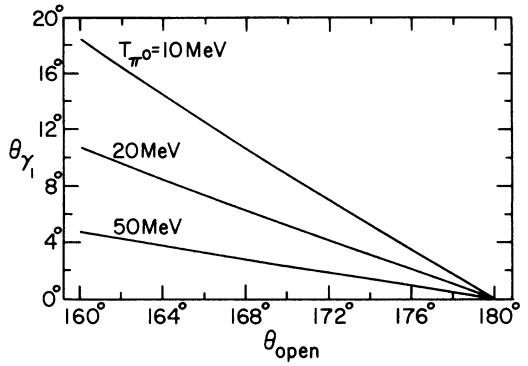


FIG. 2. Decay photon angle of emission relative to $\pi^0$ momentum for the high energy decay photon as a function of photon opening angles near 180°.

and the $\pi^0$ direction is small, ≲5°. Therefore the angular distribution of the high-energy photon reflects the $\pi^0$ angular distribution.

The experimental configuration is shown in Fig. 3. It consists of two cylindrical photon detectors viewing a target which lies on their common axis of symmetry. The high-energy photon is observed in a crude Pb-glass spectrometer while the low-energy photon is observed in a large volume NaI(Tl) spectrometer. The photon opening angle is restricted to a range of 170° to 180°, insuring that, for all but the lowest energy $\pi^0$, the high-energy photon is emitted within a few degrees of the angle of emission of the original $\pi^0$. In essence, the $\pi^0$ energy spectrum is obtained from the spectrum of photon energies observed in the NaI(Tl) detector and the $\pi^0$ angular distribution is determined from the direction of the high-energy photon observed in the Pb-glass shower counter.

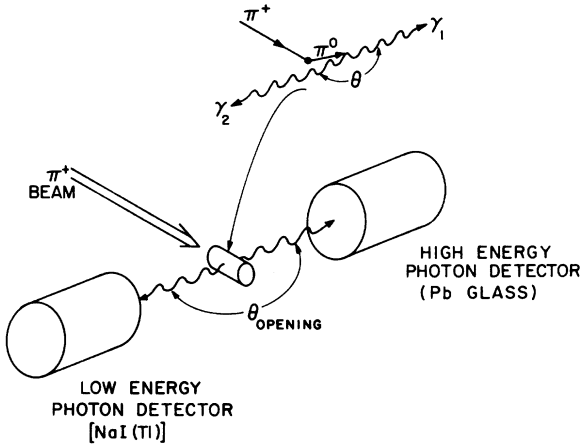


FIG. 3. Experimental configuration showing a single $\pi^0$ detector pair. The inset shows a typical event and the corresponding photon opening angle $\theta$.

An understanding of the efficiency of the detection system follows from simple kinematic features of the two photon decay. Because of the strong correlation in the directions of the high-energy decay photon and the $\pi^0$, the solid angle of the high-energy photon is essentially the solid angle of acceptance for the $\pi^0$. We can approximate the detection efficiency by the product of the probability that the $\pi^0$ is emitted within the acceptance of the Pb-glass detector times the probability that the low-energy photon is emitted in the acceptance of the second detector. One can show from the Lorentz transformation for the decay photon that the yield of photons/$\pi^0$ sr emitted near opening angles of 180° is given by

$$\frac{dN}{d\Omega} = \frac{1}{8\pi}\left(\frac{m_{\pi^0}c^2}{p_{\pi^0}c}\right)^2, \tag{1}$$

where $m_{\pi^0}$ and $p_{\pi^0}$ are the mass and momenta of the $\pi^0$. For opening angles larger than 160° this quantity is very insensitive to the actual value of the pion opening angle. For scattered $\pi^0$'s with intensity $I_{\pi^0}$ the coincident rate will be

$$N(\text{coin}) = I_{\pi^0}\Delta\Omega_1 \frac{dN}{d\Omega}\Delta\Omega_2\epsilon_2, \tag{2}$$

where $\epsilon_2$ is the photoefficiency of the NaI(Tl) detector. If we define $\epsilon$ as the probability of detecting the second photon, given observation of the first in the high-energy photon detector

$$\epsilon = \frac{1}{8\pi}\left(\frac{m_{\pi^0}c^2}{p_{\pi^0}c}\right)^2 \Delta\Omega_2\epsilon_2, \tag{3}$$

we find for $T_{\pi^0} = 100$ MeV, $\Delta\Omega_2 = 1\%$ and $\epsilon_2 = 0.5$ the detection efficiency $\epsilon \approx 10^{-3}$. Solid angles for the high-energy photon detector typical of the present experiment were in the range of ≈0.1 sr. With this solid angle an estimate gives, for example, an effective solid angle/detector pair of ≈0.1 msr at 100 MeV. This detection efficiency would result in a counting rate of the order of 500 counts/hmbsr for a $\pi$ flux of ~$10^7$ $\pi$/s. In Table I estimates of the $\pi^0$ detection efficiency based on this approximation, i.e., Eq. (2) with $\epsilon_2 = 1$, are compared with the results of a more exact numerical integration of the efficiency over the acceptance of the detector pair for various values of $\pi^0$ kinetic energy. The error generated by this approximation is never more than 2% for the geometries used in this experiment.

TABLE I. Comparison of approximate and "exact" estimates of the $\pi^0$ detection efficiency per detector pair for a geometry in which both photon detectors have effective solid angles of 0.089 sr.

| $T_{\pi^0}$ (MeV) | $pc_{\pi^0}$ (MeV) | $\Delta\Omega_{\text{approx}}$ (msr) | $\Delta\Omega_{\text{"exact"}}$ (msr) |
|---|---|---|---|
| 20 | 76.1 | 0.990 | 1.012 |
| 50 | 126.5 | 0.360 | 0.359 |
| 100 | 192.3 | 0.154 | 0.157 |
| 150 | 251.0 | 0.091 | 0.092 |
| 200 | 306.6 | 0.061 | 0.062 |

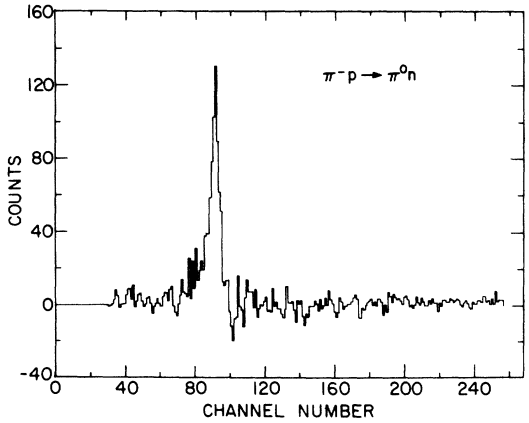


FIG. 4. Decay photon spectrum observed for neutral pions emitted at 120° in the reaction $\pi^- p \rightarrow \pi^0 n$ at 100 MeV.

Two NaI(Tl)-Pb glass detector pairs, in the configuration shown in Fig. 3, were used in the measurements. The NaI(Tl) crystals were 25 cm in diameter and 30 cm thick. They were shielded by a layer of $^6$LiH and by a plastic scintillator anticoincidence shield which was surrounded by 11 cm thick Pb shielding. The energy resolution of the spectrometers was about 3.8% for 23 MeV $\gamma$ rays (the energy corresponding to a 100 MeV $\pi^0$) when operated in the anticoincidence mode. The energy resolution and detection efficiencies of the spectrometers for $\pi^0$'s were determined by observing the reaction $\pi^- p \rightarrow \pi^0 n$. The photon spectra were obtained from the difference of data for $CH_2$ and C targets. $\pi^0$ production cross sections were calculated from known $\pi$-nucleon phase shifts. A typical low-energy photon spectrum observed for the $\pi^- p \rightarrow \pi^0 n$ reaction at $T_{\pi^-} = 100$ MeV and at an angle of 120° is shown in Fig. 4. When kinematic effects in the reaction were removed, the $\pi^0$ resolution was found to be 5.2 MeV.

The measurements were carried out using the low-energy pion channel at the Clinton P. Anderson Meson Physics Facility. The pion fluxes were approximately $2 \times 10^7$ pions/s for incident energies of 50 and 100 MeV. The profile of the beam at 50 MeV had a full width at half maximum (FWHM) = 4.0 cm horizontally and 1.4 cm vertically. The corresponding values at 100 MeV were 2.8 and 1.4 cm, respectively. The pion fluxes were determined by integrating the current generated in a

large area ion chamber placed beyond the region of the beam line viewed by the photon detectors. The flux was determined absolutely for each target and beam condition by measuring the activation due to the $^{12}C(\pi,\pi n)^{11}C$ reaction in scintillators of dimensions identical to those of the targets. Target thicknesses were ~1.0 g/cm$^2$. As stated above, the NaI(Tl) spectrometers were calibrated by using the $\pi^- p \to \pi^0 n$ reaction as a standard source. The intensity of the peak in the photon spectrum (see Fig. 4) measures the product of photoefficiency and solid angles, $\Delta\Omega_1\Delta\Omega_2\epsilon_2$ of Eq. (2) at $E_\gamma = 27$ MeV, which corresponds to a 59 MeV $\pi^0$. A seven-parameter function which describes the detector-response function over the full range of photon energies was obtained from such data. Subsequent tests of the NaI(Tl) detector using monochromatic tagged photons and photons from the $^{11}B(p,\gamma)$ reaction showed that the detector response shape $R(E)$ obtained in this way was independent of photon energy over the range 15–30 MeV when the pulse height is measured fractionally; i.e., $R(E) \equiv f(E/E_{\gamma\,\text{incident}})$. The integrated photofraction was constant to ~2%. The $\pi^0$ yields, $I(E_{\pi_0})$, were determined from the photon spectra by using Eq. (2) with $\Delta\Omega_1\Delta\Omega_2\epsilon_2$ assumed to be constant with photon energy and correcting the photon spectrum for the Jacobian relating the photon and $\pi^0$ energy scales.

## III. RESULTS

Typical $\pi^0$ spectra for the $^{16}O(\pi^+,\pi^0)$ process are shown in Fig. 5 for reaction angles of 40 and 120°. The data shown in Fig. 5 are obtained by transforming the observed $\gamma$-ray spectra without any correction for the effects of detector resolution. Data for all targets were characterized by the broad energy distributions typical of $^{16}O$ in Fig. 5. A complete set of data obtained for $^{16}O$ at 100 MeV is shown in Fig. 6. Because the NaI(Tl) spectrometer has a resolution width of approximately 5 MeV (in $\pi^0$ energy) and a response function with a small low-energy tail, it is necessary to unfold the resolution function from the measured distribution. Failure to do so would cause systematic errors when the transformation is made from the $\gamma$-ray energy to $\pi^0$ energy. We unfolded the measured resolution function using a conventional matrix inversion technique.[4] Figure 6 shows the double differential cross sections obtained as a result of this procedure. Beyond 90° we find a broad peak centered roughly at the energy appropriate to pion scattering by free nucleons (as will be evident from the discussion of the following section). These spectra suggest that charge ex-

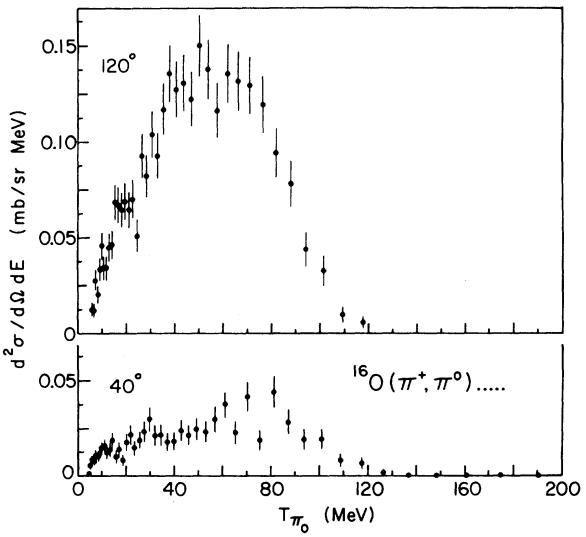


FIG. 5. Differential cross sections measured for single charge exchange by $^{16}O$ at 40 and 120°.

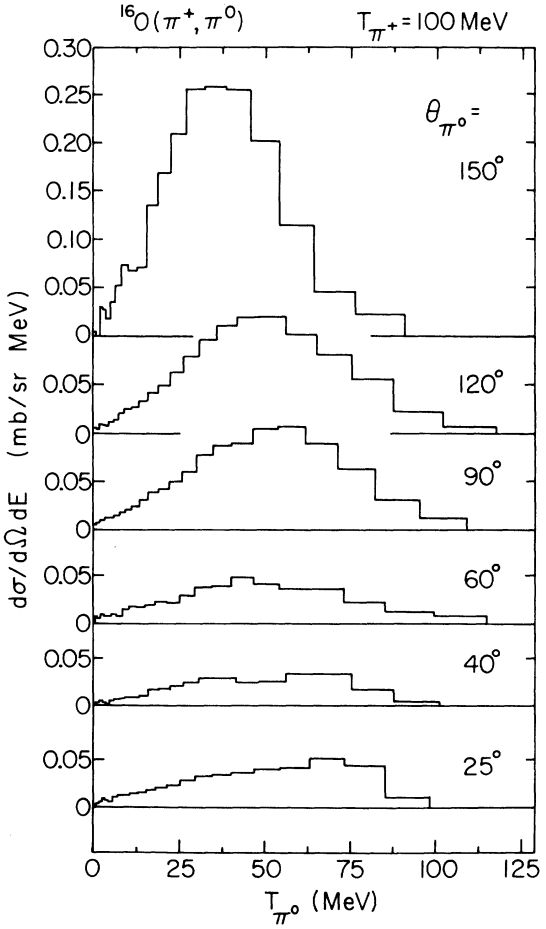


FIG. 6. Spectra of $\pi^0$ with detector resolution unfolded for incident pions with $T_{\pi^+} = 100$ MeV incident on $^{16}O$.

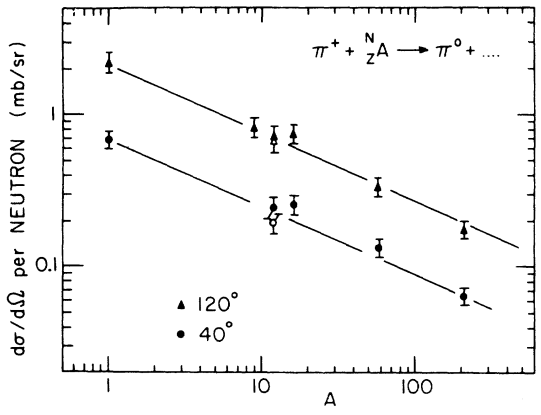


FIG. 7. Differential cross section per neutron for single charge exchange as a function of target mass. The open points for $A = 12$ were taken with negative pions.

change at large angles is dominated by quasifree scattering. However, at forward angles the energy spectra show a large $\pi^0$ yield at lower energies than one would expect from simple quasifree scattering. The spectra suggest that at forward angles, where quasifree scattering is weak, the spectra are a mixture of multistep and quasifree events.

The backward peaking observed in the $^{16}O$ data was found to be typical of all the targets studied. This interesting aspect of the data is shown in Fig. 7, where the energy integrated cross sections/target neutron observed at $\pi^0$ emission angles of 40 and 120° are presented for 100 MeV pions on a range of targets. The data indicate that the cross sections/neutron scale approximately as $A^{-0.4}$ and that the $\pi^0$ backward peaking is essentially independent of mass. The value observed for the ratio of the 40 to 120° cross section is close to that observed for the free nucleon, 3.2. The strong decrease in the cross section/neutron is consistent with strong absorption of the incident pion.

One can integrate the $\pi^0$ energy distributions to obtain total differential cross sections. The angular distribution for $^{16}O$ obtained from this integration is shown in Fig. 8. These data show that the angular distribution for nuclear charge exchange is strongly backward peaked with a distribution that is very close to that of a free nucleon. However, as we will see in the discussion below, that similarity is somewhat misleading because the energy distributions suggest that most of the cross section at forward angles is due to more complex processes than one-step quasifree charge exchange. The cross sections we observe at 50 MeV support such a conclusion. At 50 MeV the cross section for free nucleon processes fall very rapidly at forward angles. Nevertheless, as indicated

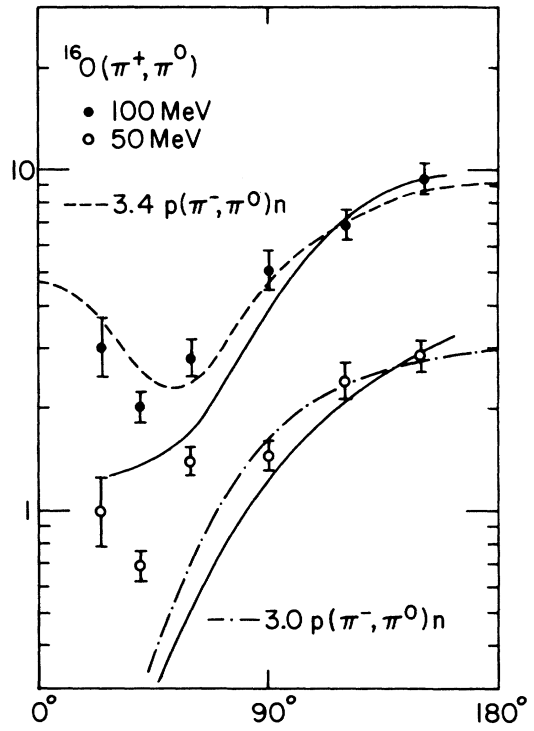


FIG. 8. Pion single-charge-exchange cross section for $^{16}O$ at 50 and 100 MeV. The dashed and dot-dashed curves represent normalized free nucleon cross sections (see text). The solid curves are the results of Fermi-gas calculations described in the text. The curves correspond to charge exchange by 4.73 and 3.27 neutrons at 50 and 100 MeV, respectively.

in the data of Fig. 8, there is experimentally a substantial cross section in the forward angle region which cannot be attributed to single-nucleon-charge exchange and which we therefore assume to be multistep charge-exchange scattering.

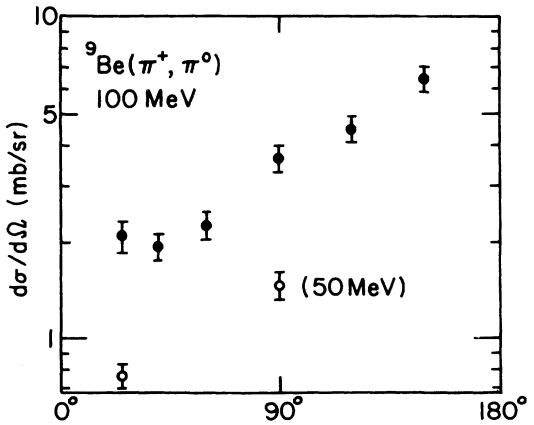


FIG. 9. Pion single-charge-exchange cross section for $^9Be$ at 100 MeV. Open circles indicate data for 50 MeV incident pions.

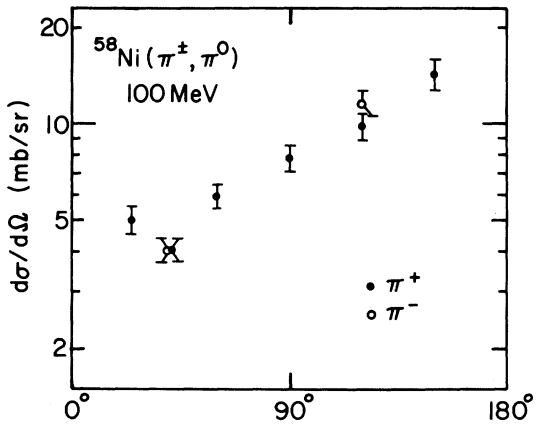


FIG. 10. Pion single-charge-exchange cross section for $^{58}$Ni at 100 MeV.

Our data for $^{9}$Be are shown in Fig. 9 for $T_{\pi^+}$ = 100 MeV. The shape is very similar to that observed for $^{16}$O. Two points, shown for incident 50 MeV $\pi^+$, indicate that, as we expect, the cross section in this mass region is changing very rapidly with energy in the same manner as the free nucleon cross section. The results for $^{58}$Ni at 100 MeV are shown in Fig. 10. Again the angular distribution is strongly backward peaked with essentially the same shape as the $^{16}$O data. Within statistical errors, the points for $\pi^+$ and $\pi^-$ are identical. This apparent independence of pion charge may reflect the fact that the reaction is largely quasifree charge exchange for which the pion charge dependence would be $\sigma(\pi^+)/\sigma(\pi^-) \approx N/Z = \frac{30}{28}$. The $\pi^0$ energy spectra have essentially the same features as those of $^{16}$O.

In Table II a compilation is presented of the integrated charge-exchange cross sections measured. We are interested among other things in knowing if single-charge exchange is an important component of the total pion reaction cross section. For the nickel isotopes, measurements in which the multinucleon removal spectra were studied by observation of pion induced nuclear $\gamma$ rays[5,6] give some estimates of the reaction cross sections. From those results we estimate that the nickel cross section at 45 MeV is approximately 1000 mb and at 220 MeV is about 1200 mb. Recently, a measurement has been made[1] in which the total transmission and effective scattering cross sections were measured for a range of nuclei in the same geometry; the absorption cross section was obtained by subtraction. The data at 125 MeV indicate that the reaction cross section for carbon is approximately 450 mb and that for Fe it is about 1100 mb. Below 130 MeV the reaction cross sections do not appear to vary rapidly with energy and consequently, from a comparison of these rough numbers with the data of Table II, we can conclude that qualitatively the charge-exchange cross sections are about 10% of the total reaction cross section.

TABLE II. Total pion charge exchange cross sections $\sigma(\pi^+,\pi^0)$ for the reaction $A(\pi^+,\pi^0)x$.

| Target | $T_{\pi^+}$ (MeV) | $\sigma(\pi^+,\pi^0)$ (mb) |
|---|---|---|
| $^{9}$Be | 100 | 45 ± 7 |
| $^{16}$O | 50 | 21 ± 3 |
| | 100 | 66 ± 10 |
| $^{58}$Ni | 100 | 104 ± 15 |

## IV. DISCUSSION

A primary objective of the measurements is to clarify the role of quasifree scattering by comparing the $\pi^0$ angular distributions and energy spectra with those which characterize the $\pi$-nucleon reaction. We have carried out a series of simple calculations to determine what the expected properties of quasifree charge exchange would be. The dashed curves of Fig. 8 show the differential cross sections for the $n(\pi^+,\pi^0)p$ reaction in the nucleon rest frame calculated from known $\pi$-nucleon phase shifts[7] and normalized to the back-angle data points. Interference between $s$ and $p$ partial waves below the $\Delta(3,3)$ resonance produces the backward peaking which characterizes the curves for 50 and 100 MeV pions. As the $\Delta(3,3)$ resonance energy is approached, the reaction becomes forward peaked. Of course, in nuclear matter these distributions will be distorted by effects due to absorption and Pauli blocking, particularly in the forward direction. Two separate calculations which include Fermi broadening were performed. The first calculation using a Fermi-gas model similar to that of Moniz[8] was made for $(\pi^+,\pi^0)$ scattering by $^{16}$O. The results are given by the solid curves in Fig. 8. Pauli blocking, as expected, reduced the cross section at forward angles much more than at the larger angles. This effect can be gauged by comparing the dashed and solid curves in Fig. 8. The calculation shown in Fig. 8 was normalized to the data at an angle of 150°. This normalization leads to an effective neutron number of 4.73 at $T_{\pi^+}$ = 50 MeV and 3.27 at 100 MeV. This effective neutron number should not be confused with those obtained in free-nucleon calculations in which Pauli blocking has not been taken into account. Clearly, the Fermi-gas calculation is much too simple to explain the measured angular distribution. The results of a second calculation for $T_{\pi^+}$ = 100 MeV of charge ex-

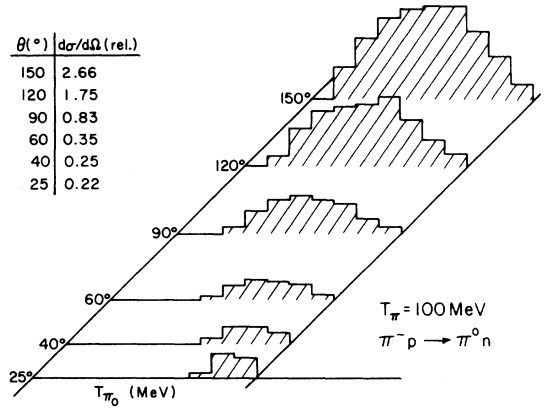


FIG. 11. Energy distributions of $\pi^0$ at selected emission angles resulting from charge exchange by a zero temperature neutron-proton Fermi gas.

change by free nucleons which were assumed to have a Fermi motion with $P_F = 270$ MeV/$c$ is shown in Fig. 11. The energy and angular distribution of the differential cross sections were deduced from $\pi$-nucleon phase shifts and the effects of Pauli blocking are included in the computation. As indicated in Fig. 11, beyond 90° Fermi broadening produces an energy spectrum that spans essentially the complete range of allowed energy transfers. Pauli blocking reduces the scattering at forward angles. The energy integrated cross sections resulting from this Fermi-broadened free nucleon gas calculation are tabulated in Fig. 11. There is very little difference in the shape of the energy spectra for the two calculations. Of course such simple calculations using the infinite nuclear matter density probably overestimate the nuclear binding effects.

In general, the picture of single-charge exchange as mainly quasifree $\pi$-nucleon charge exchange with a small component of multistep reactions does appear to be qualitatively consistent with our data. Multistep reactions appear to be a major component of the $\pi^0$ spectrum only at forward angles where the quasifree process is small. Because the angular distributions are backward peaked, the total cross section arises mostly from quasifree scattering. This can best be demonstrated by comparing the data of Fig. 6 for $^{16}O(\pi^+, \pi^0)$ with the results of the Fermi-gas calculation shown in Fig. 11. At back angles the spectrum has a shape characteristic of quasifree scattering. At 40° much of the yield corresponds to energy losses too large to be quasifree scattering. It is interesting to note, however, that if one takes only the portion of the 40° spectrum that is in the expected quasifree scattering region, then the resulting cross section is consistent with our simple calculations. This indicates that the quasifree portion of the charge-exchange scattering at forward angles is inhibited by Pauli or absorption effects.

The total charge-exchange cross sections inferred from our data can provide tests of current optical model potentials used to describe pion-nucleus scattering. Indeed, Thomas and Landau[9] have pointed out that a correct prediction of the quasifree scattering is important in assessing the validity of any description of pion-nucleus elastic scattering. In the absence of such a requirement, the strength of true absorption and quasifree scattering are unconstrained, and resulting optical potentials, while describing correctly elastic scattering, would be unreliable for discussing inelastic channels or estimating nuclear size parameters. We have seen that the charge-exchange reaction is predominately quasifree scattering. Since charge exchange arises solely from the isovector term, its observation and comparison with the total inelastic pion scattering should put some constraint on the isospin structure of the optical model.

Table III shows data for $^{16}O$. The total single-charge-exchange cross sections were obtained by integrating the corresponding angular distributions. It is of interest to check their consistency under reasonable assumptions with the limited data available on total inelastic scattering cross sections. To do this we have estimated the inelastic cross section $\sigma(\pi, \pi')$ by multiplying our measured charge-exchange cross section by the ratio of the sum of the free proton and neutron cross sections to the corresponding free nucleon charge-exchange cross section evaluated at each pion energy. Using this procedure with the actual free nucleon cross sections gives a ratio which is significantly below the value of 5 predicted by $\Delta(3,3)$ dominance in this energy range. The only data available is that of Ingram *et al.*,[10] who observe for $\sigma(\pi, \pi')$ on $^{16}O$ 224 ± 30 and 291 ± 40 mb at 115 and 165 MeV. Our inferred data for $\sigma(\pi, \pi')$ appear to be ~20% higher when allowance is made for differences in the incident pion energies. This departure from the ratio predicted from the free nucleon cross sections may be due in part to the presence of multistep processes in

TABLE III. Measured total single pion charge-exchange cross sections and estimated total inelastic scattering cross sections.

| Target | $T(\pi^+)$ MeV | $\sigma(\pi^+, \pi^0)$ mb | $\sigma(\pi^+, \pi^{+\prime})$ [a] | $\sigma(\pi^+, \pi^{+\prime}) + \sigma(\pi^+, \pi^0)$ mb |
|---|---|---|---|---|
| $^{16}O$ | 50 | 21 | 47 | 68 |
| | 100 | 66 | 254 | 320 |

[a] Calculated by using the ratio $R = [\sigma(\pi^+ p \rightarrow \pi^+ p) + \sigma(\pi^+ n \rightarrow \pi^+ n)]/\sigma(\pi^+ n \rightarrow \pi^0 p)$ for the free nucleon values at $T_\pi$.

TABLE IV. Quasifree (q.f.) and total reaction cross sections from optical model calculations.

| Target | $T(\pi^+)$ (MeV) | $\sigma_T^{q.f.}(\pi,\pi'+\pi,\pi^0)$ (mb) | $\sigma_{react}$ (mb) |
|---|---|---|---|
| $^{16}O$ | 50 [a] | 45 | 201 |
| $^{16}O$ | 40 [b] | | 132 |
| | 79 [b] | | 376 |
| | 114 [b] | | 492 |

[a] Reference 12.
[b] Reference 13.

the $(\pi^+,\pi^0)$ reaction. Arguments[11] based on pion nucleon cross sections suggest multistep reactions should be stronger relative to quasifree scattering in the charge-exchange reaction as compared to inelastic scattering.

In a first order optical model the cross sections for simple inelastic pion scattering and for pion-charge exchange have the same ratio as the corresponding sum of pion nucleon cross sections. Therefore as a point of comparison with optical-model predictions we have chosen the total pion nonelastic scattering cross section $\sigma(\pi^+,\pi^{+\prime})$ $+\sigma(\pi^+,\pi^0)$. In Table IV several pertinent optical-model results are given. Stricker, McManus, and Carr[12] estimate a quasifree cross section for $^{16}O$ at 50 MeV, which is substantially less than the value estimated from the present experimental data. Although Liu and Shakin[13] do not estimate directly the quasifree component, they do give estimates of the total reaction cross sections. Our estimates of total scattering in Table III appear large compared to these reaction cross sections when it is noted that other experiments[14] indicate that pion absorption is a large part of the reaction cross section in this region. Although the data are very limited, it appears that the estimated nonelastic scattering cross sections are roughly 50% larger than values inferred from optical potentials. We interpret this as an indication that the charge-exchange cross sections from which they are calculated are 1.5 times the values that would be predicted by the optical model.

It has been suggested[15] that "soft pion" charge-exchange effects could alter the ratio between charge exchange and total quasifree scattering in a manner similar to the way nucleon charge exchange affects the $\pi^-/\pi^+$ ratio for the $^{12}C(\pi,\pi n)^{11}C$ cross sections. In this picture, soft pion charge exchange occurs on the pion before or after the "hard" quasifree scattering in such a way as to preserve the pion direction and energy. Because the direct inelastic scattering is so much stronger than the charge-exchange scattering, a small "soft" exchange would drastically alter the relative strength of the $\pi^0$ reaction. Silbar used a semiclassical pion transport theory to estimate the increase expected, and found that the enhancement could be as much as a factor of 2. However, there are two reasons why the semiclassical calculation may give an overestimate of the "soft pion" charge-exchange effect. First, it does not allow for the strong backward peaking of the basic $\pi^+ n \to \pi^0 p$ reaction at 100 MeV and second, Pauli-blocking effects, which will further inhibit forward scattering, are not included. Both of these effects will be strongest for the soft scattering which preserved the direction and energy of the incident pion. Therefore, it does not appear that soft pion second chance reactions account for the enhancement. More detailed calculations are needed to confirm this point.

## V. SUMMARY

In conclusion, the $\pi^0$ angular distributions and energy spectra measured in the energy range 50–100 MeV indicate that pion-nucleus charge exchange favors large momentum transfer. The quasifree process appears to play a major role in inclusive-charge exchange. A crude analysis based on free nucleon cross sections indicates that total nonelastic scattering cross sections are ~1.5 times values suggested by optical model calculations. Measurements extending observations to higher pion energies where the angular distributions become forward peaked will be particularly useful in confirming the role of quasifree scattering. More data are needed both for charge exchange and inelastic pion scattering. Such information will provide rigorous tests of optical model potentials and the isospin structure of the interaction.

This work was performed under the auspices of the U. S. Department of Energy and the National Science Foundation.

*Present address: Los Alamos Scientific Laboratory, Los Alamos, New Mexico 87545.
†Present address: DPhN/ME, CEN Saclay, 91190 Gif-sur-Yvette, France.
‡Present address: Department of Physics, University of Illinois, Urbana, Illinois 61801.
§Present address: Indiana University Cyclotron Facility, Bloomington, Indiana 47401.
||Present address: Schlumberger Well Services, Houston, Texas 77000.

[1]I. Navon, D. Ashery, G. Azuelos, H. J. Pfeiffer, H. K. Walter, and F. W. Schleputz, Phys. Rev. Lett. 42, 1465 (1979).
[2]Limited information on total cross sections at 70 MeV exists. See H. Hilscher, W. D. Krebs, G. Sepp, and V. Soergel, Nucl. Phys. A158, 602 (1970).
[3]T. Bowles, D. F. Geesaman, R. J. Holt, H. E. Jackson, R. M. Laszewski, J. R. Specht, L. L. Rutledge, Jr., R. E. Segel, R. P. Redwine, and M. A. Yates-Williams, Phys. Rev. Lett. 40, 97 (1978).
[4]J. E. Monahan, in *Scintillation Spectroscopy of Gamma Radiation*, edited by S. M. Shafroth (Gordon and Beach, London, 1967), Vol. 1, Chap. VIII, pp. 371–428.
[5]Y. Cassagnou, H. E. Jackson, J. Julien, R. Legrain, and L. Roussel, Phys. Rev. C 16, 741 (1977).
[6]H. E. Jackson, S. B. Kaufman, D. G. Kovar, L. Meyer-Schützmeister, K. E. Rehm, J. P. Schiffer, S. L. Tabor, S. E. Vigdor, and T. P. Wangler, Phys. Rev. C 18, 2656 (1978).
[7]M. Salomon, Low Energy Pion-Nucleon Phase-Shift Fits, TRIUMF Report No. Tri-74-2, 1974 (unpublished).
[8]E. J. Moniz, Phys. Rev. 184, 1154 (1969).
[9]A. W. Thomas and R. H. Landau, Phys. Lett. 77B, 155 (1978).
[10]C. H. Q. Ingram, J. Bolger, E. T. Boschitz, G. Pröbstle, J. A. Jansen, J. Zichy, P. A. M. Gram, R. E. Mischke, and J. Arvieux (unpublished).
[11]C. H. Q. Ingram, *Meson-Nuclear Physics–1979 (Houston)*, Proceedings of the 2nd International Topical Conference on Meson-Nuclear Physics, edited by E. V. Hungerford III (A.I.P., New York, 1979), p. 49.
[12]K. Stricker, H. McManus, and J. A. Carr, Phys. Rev. C 19, 929 (1979).
[13]L. C. Liu and C. M. Shakin, Phys. Rev. C 19, 129 (1979).
[14]D. Ashery, Nucl. Phys. A335, 385 (1980).
[15]R. R. Silbar, LAMPF Workshop on Pion Single Charge Exchange, Report No. LA-7892C, 339, 1979 (unpublished).